PCCP

RSC Publishing

PAPER

View Article Online
View Journal | View Issue

Cite this: *Phys. Chem. Chem. Phys.*, 2013, **15**, 18445

Do H-bonds explain strong ion aggregation in ethylammonium nitrate + acetonitrile mixtures?†

Thomas Sonnleitner,[a] Viktoriya Nikitina,[b] Andreas Nazet[a] and Richard Buchner*[a]

Received 25th April 2013,
Accepted 13th August 2013

DOI: 10.1039/c3cp51773j

www.rsc.org/pccp

Binary mixtures of the protic ionic liquid ethylammonium nitrate (EAN) and acetonitrile (AN) were studied at 25 °C over the entire composition range by means of broadband dielectric spectroscopy covering $0.2 \leq \nu/\mathrm{GHz} \leq 89$. The dielectric spectra could be decomposed into two relaxation processes, both of which proved to be composite modes. For dilute solutions the higher-frequency Debye relaxation centered at ~60 GHz is associated with the rotational diffusion of AN molecules, whereas at higher salt concentrations ultra-fast intermolecular vibrations and librations of EAN dominate the process. For EAN-rich solutions the lower-frequency relaxation is mainly due to jump reorientation of the ethylammonium cation, whereas contact ion pairs (CIPs) dominate this mode for dilute solutions. From the relaxation amplitudes effective solvation numbers and ion-pair concentrations were determined. For vanishing EAN mole fraction, $x_{EAN} \rightarrow 0$, an effective cation solvation number of ~7 was found which steeply drops until $x_{EAN} \approx 0.2$ but shows only moderate decrease later on. The obtained association constant for EAN, K_A^0 = 970 L mol^{-1}, exceeds that of other 1 : 1 electrolytes in AN by a factor of ~30–50. This observation, as well as the fact that CIPs are formed despite strong cation solvation, indicates that ion pairing is mainly driven by the formation of strong hydrogen bonds between anions and cations.

1 Introduction

Ionic liquids (ILs) are salts with a melting point below 100 °C.[1] Protic ionic liquids (PILs), formed by proton exchange from a Brønsted acid to a Brønsted base, are a particular sub-group that has gained increasing attention during recent years.[2] The key property of PILs is their relatively high electrical conductivity caused by fast proton transfer, which makes them particularly interesting for applications in batteries and fuel cells.[2,3] Probably the most intensively studied PIL is ethylammonium nitrate (EAN). Due to its ability to form a three dimensional hydrogen bond network reminiscent of water,[4,5] it has attracted particular interest as possible replacement for aqueous solutions in organic synthesis[2] and as self-assembling medium.[4,6,7,8]

In practical applications ILs are generally mixed with other components, either acting as co-solvents or as reactants. To understand interactions in such systems knowledge of their structure and dynamics is essential. Up to now, most publications dealing with the dynamics of ILs and their mixtures with non-ionic compounds have focused on salts with 1-alkyl-3-methylimidazolium cations[9–13] but only little is known about PIL-containing systems.[14,15] In this contribution we present a first systematic study of the cooperative dynamics of EAN + dipolar aprotic solvent mixtures. Acetonitrile (AN) was chosen as the non-ionic component as this industrially important solvent[16,17] is miscible with EAN over the entire composition range. Additionally, its structure and dynamics are well characterized.[18–21]

As the main technique dielectric relaxation spectroscopy (DRS) was used as it has proven to be a powerful tool for studying the dynamics of electrolyte solutions[22–24] and ILs.[12,25,26] DRS measures fluctuations of the macroscopic dipole moment of the sample and is therefore sensitive to the reorientation of dipolar species in general and to ion pairs in particular.[24] Furthermore, this technique yields information on solute–solvent interactions and is the only method allowing determination of the static permittivity of conducting samples. Note that the frequency-dependent dielectric properties of a solvent also determine how fast and efficient it can respond to changes in the charge distribution of a solute, affecting thus fast photochemical and electron transfer reactions therein.[27,28]

2 Experimental

2.1 Materials and auxiliary measurements

Ethylammonium nitrate (EAN, >97% purity) was purchased from Iolitec (Heilbronn, Germany) and dried under vacuum

[a] *Institute of Physical and Theoretical Chemistry, Universität Regensburg, 93053 Regensburg, Germany. E-mail: Richard.Buchner@chemie.uni-regensburg.de*
[b] *Department of Electrochemistry, Moscow State University, Moscow, Russian Federation*

† Electronic supplementary information (ESI) available: Tables with the fit parameters of the dielectric spectra (amplitudes, relaxation times, *etc.*) and of density, conductivity and viscosity of EAN + AN mixtures. See DOI: 10.1039/c3cp51773j

($p < 10^{-8}$ bar) for 12 days at 40 °C. This reduced the water content to <100 ppm as measured by coulometric Karl Fischer titration. Acetonitrile (anhydrous, VWR Prolabo, Darmstadt, Germany) had a nominal water content of <30 ppm and was used as received. Both EAN and AN were stored in a nitrogen-filled glove-box and all subsequent steps of sample preparation and measurements were performed under dry nitrogen. EAN + AN mixtures were prepared using an analytical balance without buoyancy corrections and thus were accurate to about ±0.2%.

Densities, ρ, required for calculating the molar concentrations of EAN, c_{EAN}, and AN, c_{AN}, were measured at (25.00 ± 0.01) °C using a vibrating-tube densimeter (Anton Paar, Graz, Austria, DMA 5000 M) with a nominal uncertainty of $\pm 5 \times 10^{-6}$ g cm^{-3}. Viscosities, η, measured at (25.00 ± 0.05) °C were obtained with the help of an automated rolling ball microviscometer (Anton Paar, Graz, Austria, AMVn) having a repeatability of ~0.5%. Electrical conductivities, κ, were determined at (25.000 ± 0.003) °C with an overall uncertainty of 0.5% using the setup described previously.[29,30] The obtained data for ρ, κ, molar conductivity, $\Lambda = \kappa/c_{EAN}$, and η are summarized in Table S1 (ESI†).

2.2 Dielectric spectroscopy

Dielectric relaxation spectroscopy (DRS) probes polarization as the linear response of the sample to a time-dependent electric field, which corresponds to fluctuations of the macroscopic dipole moment[24,31] In the frequency domain, the experimentally accessible quantity is the complex generalized permittivity

$$\hat{\eta}(\nu) = \hat{\varepsilon}(\nu) - i\kappa/(2\pi\nu\varepsilon_0) \quad (1)$$

at frequency, ν, where the dc conductivity κ characterizes the Ohmic loss arising through the steady-state migration of ions in the applied electric field; and ε_0 is the permittivity of free space. All frequency(time) dependent rotational, vibrational and translational contributions are summarized in the complex relative permittivity.

$$\hat{\varepsilon}(\nu) = \varepsilon'(\nu) - i\varepsilon''(\nu) \quad (2)$$

Typical for relaxation phenomena, the relative permittivity, $\varepsilon'(\nu)$, shows dispersion from the static permittivity, $\varepsilon_s = \lim_{\nu\to 0}\varepsilon'(\nu)$, where polarization is at equilibrium with the external field, to the "infinite-frequency" limit $\varepsilon_\infty = \lim_{\nu\to\infty}\varepsilon'(\nu)$, where dipole fluctuations are unable to follow. Simultaneously, energy dissipation characterized by the dielectric loss, $\varepsilon''(\nu)$, arises from the coupling of electromagnetic waves to dipole fluctuations.[32]

Dielectric spectra were recorded in the frequency range of $0.2 \le \nu/\text{GHz} \le 89$ at (25.00 ± 0.05) °C. For $0.2 \le \nu/\text{GHz} \le 50$ a dielectric probe kit consisting of two reflection probe heads (Agilent 85070E-020 for 0.2–20 GHz and Agilent 85070E-050 for 1.0–50 GHz) was connected to a vector network analyzer (VNA, Agilent E8364B) *via* an electronic calibration module (ECal, Agilent N4693A).[33,34] Prior to measurement the probes were calibrated with air, mercury and *N*,*N*-dimethylacetamide (DMA) as primary calibration standards. To account for calibration errors a complex Padé-correction was applied using AN, benzonitrile and 1-butanol as secondary standards.[35] For selected samples the Padé-correction was assessed with the help of a variable-pathlength waveguide transmission cell covering $27 \le \nu/\text{GHz} \le 40$ that was mounted on the VNA as such measurements do not require calibration.[33,36] The 60–89 GHz region was covered with a waveguide interferometer.[36] The combined $0.2 \le \nu/\text{GHz} \le 89$ spectra of $\hat{\eta}(\nu)$ were then corrected for dc conductivity to extract $\hat{\varepsilon}(\nu)$ for further processing. In this procedure κ was treated as an adjustable parameter with the experimental data as the starting values to account for fringing-field contributions arising from geometrical imperfections of the VNA probes.[24]

In order to extract molecular-level information from DR spectra an appropriate relaxation model has to be found for the experimental data. Dipole fluctuations taking place at microwave frequencies for liquids at room temperature are typical relaxation processes. The associated spectra can be usually modeled by sums of n individual modes of amplitude, S_j, and relaxation time, τ_j,

$$\hat{\varepsilon}(\nu) = \varepsilon_\infty + \sum_{j=1}^{n} \frac{S_j}{\left[1 + (i2\pi\nu\tau_j)^{1-\alpha_j}\right]^{\beta_j}} \quad (3)$$

using for the individual components, j, the empirical Havriliak–Negami (HN) equation with shape parameters $0 \le \alpha_j < 1$ and $0 < \beta_j \le 1$, or its simplified variants, the Cole–Cole (CC, $\beta_j = 1$), Cole–Davidson (CD, $\alpha_j = 0$) and Debye (D, $\alpha_j = 0$, $\beta_j = 1$) equations. The static relative permittivity of the sample is given by $\varepsilon_s = \sum S_j + \varepsilon_\infty$. In addition to *intramolecular* polarizability, the present values for the infinite-frequency permittivity, ε_∞, also incorporate a small contribution from *intermolecular* librations in the THz range.

Real and imaginary parts of the present $\hat{\varepsilon}(\nu)$ spectra were simultaneously fitted using a home-built procedure implemented with the commercial IGOR software (Wavemetrics, V.6.22A). All reasonable relaxation models up to $n = 4$ were tested, including fits with inertia-corrected (superscript ^{i}) variants of the HN, CD and D equations.[37] The fits were assessed by their values of the reduced error function, χ_r^2, and the smooth concentration dependence of the obtained parameters.

3 Results and discussion

3.1 Choice of fit model

In the frequency range of 0.2–89 GHz the dielectric spectrum of neat AN at 25 °C is very well fitted by a single Debye (D) equation centered at ~48 GHz (parameters $S = 32.51$, $\tau = 3.32$ ps, $\varepsilon_\infty = 3.33$). This mode is associated with the rotational diffusion of AN dipoles[18,22] and accounts for ~95% of the total dispersion from $\varepsilon_s = 35.84$ at $\nu \to 0$ to $\varepsilon_\infty^{FIR} = 1.81$ in the far infrared so that the small resonance-type processes outside the present frequency range at ~0.5 and 2 THz[13,18,19] can be neglected in the present analysis. On the other hand, two modes (the CD^i + D model) are required to fit $\hat{\varepsilon}(\nu)$ of pure EAN in the same frequency range, see Table S2 (ESI†) for the parameters. This spectrum is dominated by the jump relaxation of $[EtNH_3]^+$ ions[26,38] peaking at ~1 GHz which is best described by an inertia-corrected[37] CD equation with a 5 THz rise rate. Additionally, a small

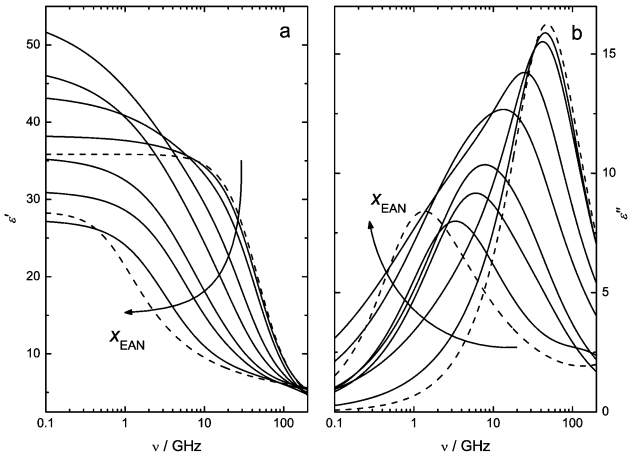

Fig. 1 (a) Dielectric permittivity, $\varepsilon'(\nu)$, and (b) loss, $\varepsilon''(\nu)$, spectra of neat AN and EAN (dashed lines) and EAN + AN mixtures with x_{EAN} of 0.0312, 0.1167, 0.2398, 0.4002, 0.5017 and 0.6989 (solid lines) at 25 °C.

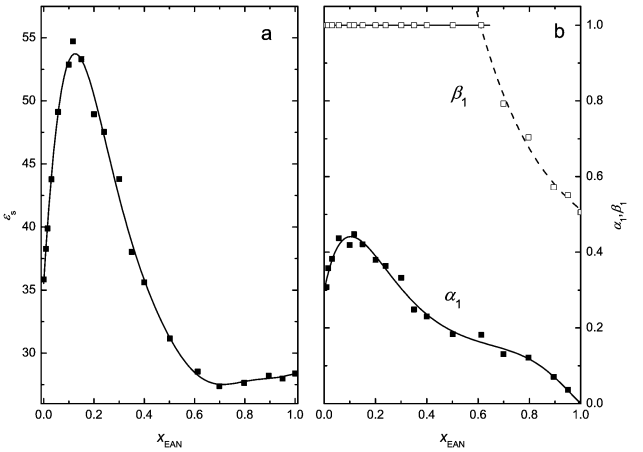

Fig. 3 (a) Static permittivity, ε_s, and (b) width parameters α_1 (■) and β_1 (□). Solid and dashed lines are just a guide to the eye.

high-frequency D equation peaking outside the present frequency range is required to summarize the small contributions from intermolecular vibrations and librations at THz frequencies that extend below 89 GHz.[26]

Data analysis revealed that for all mixture spectra a sum of two modes (n = 2 in eqn (3)) yielded the best fit (Fig. 1 and 2). Up to IL mole fractions of x_{EAN} = 0.61, a CC + D model was sufficient but above that concentration the shape of the lower-frequency mode becomes increasingly asymmetric ($\beta_1 < 1$; Fig. 3b), so that a HN^i + D model had to be used. For the HN^i mode the inertial rise rate was fixed to the value of pure EAN, 5 THz. The so obtained parameters (ESI,† Table S2) vary smoothly with x_{EAN} over the entire mixture range (Fig. 3–7). The other tested models generally produced inferior fits and/or widely scattering parameters and were thus rejected. Note that this empirical decomposition of the dielectric spectra has to be taken with a grain of salt as computer simulations of Schröder *et al.*

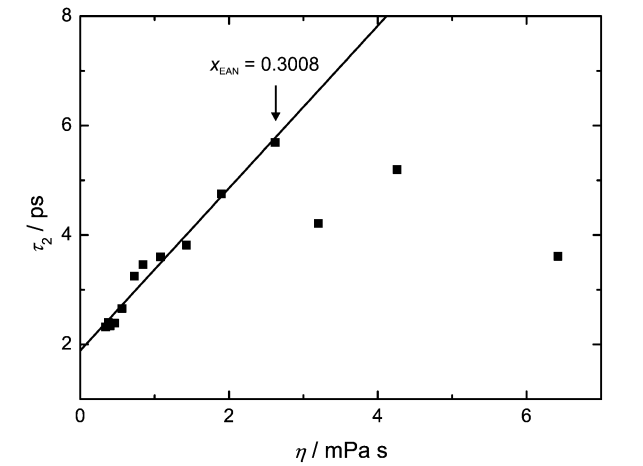

Fig. 4 Dielectric relaxation time, τ_2 (■), as a function of solution viscosity, η.

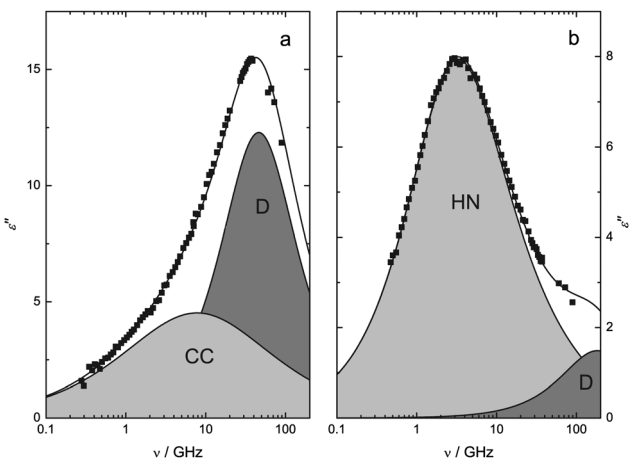

Fig. 2 Dielectric loss spectra, $\varepsilon''(\nu)$, of EAN + AN mixtures at 25 °C and EAN mol fractions, x_{EAN}, of (a) 0.0312 and (b) 0.6989. Symbols represent experimental data, lines show (a) the CC + D and (b) the HN^i + D fit; shaded areas indicate the individual processes.

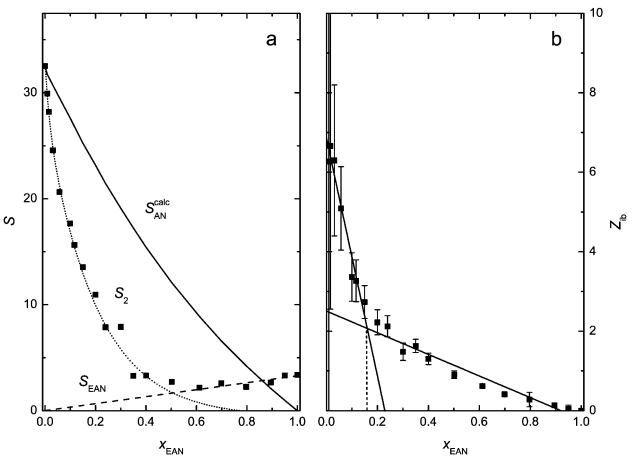

Fig. 5 (a) Observed amplitudes, S_2 (■), of mode 2 and (b) effective solvation numbers, Z_{ib}, as a function of EAN mole fraction, x_{EAN}. In (a) the full line shows the expected AN amplitude, S_{AN}^{calc}; the dashed line represents the contribution of EAN, S_{EAN}, to S_2, assumed to increase linearly with x_{EAN}, and the dotted line indicates the contribution of ''free'' AN, S_{AN}. Solid lines in (b) indicate linear fits.

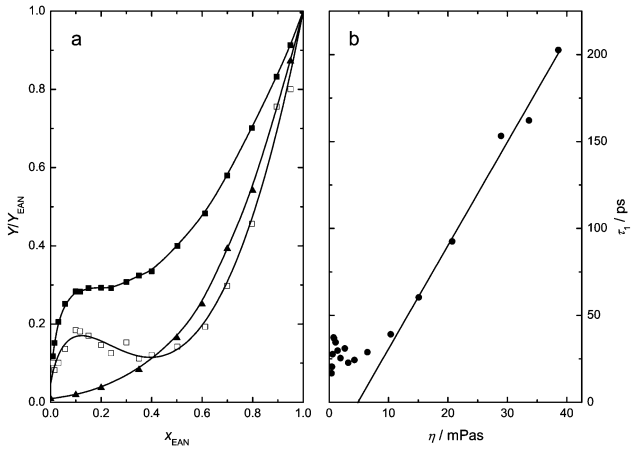

Fig. 6 (a) Normalized transport quantities, Y/Y_{EAN}, of EAN + AN mixtures at 25 °C with $Y = \tau_1$ (relaxation time of mode 1; □), $Y = \eta$ (solution viscosity; ▲) and $Y = \Lambda^{-1}$ (reciprocal molar conductivity; ■) where Y_{EAN} is the corresponding quantity of neat EAN. Lines are visual guides only. (b) Relaxation time τ_1 (●) as a function of viscosity, η, with linear fit (solid line) for $0.7 \leq x_{EAN} \leq 1$.

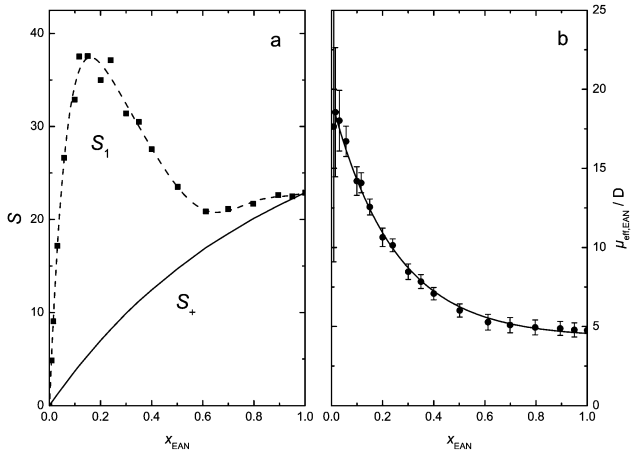

Fig. 7 (a) Amplitude of the lower-frequency mode, S_1 (■), of EAN + AN mixtures at 25 °C and predicted amplitude, S_+ (solid line), if only $[EtNH_3]^+$ cations would contribute. (b) Effective dipole moment, $\mu_{eff,EAN}$ (●), calculated from S_1 and c_{EAN} using eqn (5). The solid line represents an exponential fit; error bars correspond to the standard error ($\sigma(S_1) = 1.1$) for the polynomial fit of S_1 (broken line in (a)).

have clearly shown that at least for imidazolium-based ionic liquids and their mixtures with water rotational and translational modes of all components stretch over large frequency ranges and strongly overlap.[39–41] However, as long as quantitative agreement between experimental and simulated dielectric spectra cannot be routinely achieved empirical decompositions, like the present CC + D or HN^i + D models, have to be used.

Compared to mixtures of 1-alkyl-3-methylimidazolium ILs with AN[13] and dichloromethane (DCM),[11,42] where the spectra can be fitted with a CC + D model, some similarities but also marked differences are apparent. From the evolution of the resolved amplitudes and relaxation times it is obvious that for all mixtures studied so far, including the present EAN + AN system, the lower-frequency mode (1) is associated with the IL. At low IL content the higher-frequency mode (2) is dominated by the dipolar solvent (AN or DCM) but at $x_{IL} \gtrsim 0.5$ essentially only the IL contribution remains. All mixtures exhibit a maximum in the static permittivity at low IL content, which is an indication of ion-pair formation.[11,13,42] However, whilst only a small increase was observed for the static permittivity of imidazolium IL + AN mixtures, followed by a monotonic decrease to the value of the pure IL, the present mixtures show a huge rise from $\varepsilon_s = 35.84$ for pure AN to 54.71 at $x_{EAN} = 0.12$ (Fig. 3a). This suggests considerable formation of a species with large dipole moment, namely contact ion pairs (CIPs, see below) for $0 < x_{EAN} \lesssim 0.5$. Interestingly, the static permittivity shows also a weak minimum at $x_{EAN} \approx 0.7$, the composition where the transition from the CC + D to the HN^i + D model occurs (Fig. 3).

3.2 Higher frequency mode

3.2.1 Relaxation times. The concentration dependence of relaxation time, τ_2 (Fig. 4), and amplitude, S_2 (Fig. 5a), reveals that at low IL content the higher-frequency mode 2 is associated with the reorientation of AN dipoles. Information on the underlying relaxation mechanism comes from the corresponding rotational correlation time, τ_2', obtained from the cooperative relaxation time τ_2 with the help of the Powles–Glarum equation[43]

$$\tau_2' = \left(\frac{2\varepsilon_2 + \varepsilon_\infty}{3\varepsilon_2}\right) \times \tau_2 \qquad (4)$$

where $\varepsilon_2 = \varepsilon_s - S_1$. For $x_{EAN} \leq 0.3$ τ_2' is proportional to viscosity, η (Fig. 4), suggesting that in this region, corresponding to IL concentrations $c_{EAN} \lesssim 4.8$ M, solvent relaxation is through rotational diffusion of individual dipoles. This is typical for electrolyte solutions in dipolar aprotic solvents.[13,22,44] For $x_{EAN} \geq 0.3$ the linear relation between τ_2' and η breaks down, suggesting a rapid decrease of "freely" rotating AN dipoles and increasing dominance of fast EAN modes.

From the slope of the linear range of Fig. 4 the very small effective volume, $V_{eff} = V_m f_\perp C$, of 2.02 Å^3 can be extracted.[45] For values of $V_m = 43.9$ Å^3 and $f_\perp = 1.208$ taken as the molecular volume and the shape factor of the AN molecule[46,47] this results in a friction coefficient of $C = 0.038$. Similar small values were found for AN solutions of 1-alkyl-3-methylimidazolium tetrafluoroborates ($C = 0.033$),[13] NaI (0.063) and Bu_4NBr (0.068).[22] On the other hand, from the temperature dependence of the relaxation time of pure AN a value of $C = 0.119$ was obtained,[18] which is virtually identical to the theoretically predicted friction factor for rotation under slip hydrodynamic boundary conditions, $C_{slip} = 1 - f_\perp^{2/3} = 0.118$.[45] As argued previously,[13,24] this indicates that for dipolar aprotic solvents, like AN, the rise of solution viscosity with salt/IL content is essentially due to mixing particles of different size, *i.e.* a mere blocking effect. Long-range electrostatic interactions are only of minor importance for the viscosity of such systems. Although ion solvation occurs in the present mixtures and manifests in "freezing" AN molecules adjacent to the cations, see below, it appears that the influence of the ions on solvent rotational dynamics is limited to their first solvation shell. It is interesting to note that this

simple behaviour prevails up to x_{EAN} = 0.3, *i.e.* almost a 1 : 1 ratio of ions to solvent molecules.

3.2.2 Amplitudes. For dipole mixtures where the modes resolved in the dielectric spectrum can be assigned to individual species the Cavell equation

$$\frac{2\varepsilon_s + 1}{\varepsilon_s} S_j = \frac{N_A}{k_B T \varepsilon_0} c_j {\mu_{eff,j}}^2 \quad (5)$$

relates the amplitude, S_j, of mode j to the concentration, c_j, and the effective moment, $\mu_{eff,j}$, of the dipole.[48,49] In the derivation of eqn (5) a spherical cavity field was assumed; k_B, T and ε_0 have their usual meanings.

From the amplitude of pure AN, S_2 = 32.51 (ESI,† Table S2), and its density and molar mass the effective dipole moment of $\mu_{eff,AN}$ = 4.34 D was obtained. Assuming that this value applies for the entire mixture range, the expected AN amplitude, S_{AN}^{calc}, shown as the solid line in Fig. 5a was obtained from the analytical AN concentration, c_{AN} of the mixtures. Except for $x_{EAN} > 0.9$, S_{AN}^{calc} always exceeds the experimentally determined amplitude S_2, indicating that at least at low IL content only part of the AN is detected by DRS.

The DRS detectable (apparent) AN concentration, c_{AN}^{app}, can be calculated using eqn (5) from the EAN corrected amplitude of mode 2, $S_{AN} = S_2 - S_{EAN}$ (dotted line in Fig. 5a), assuming $S_{EAN} = x_{EAN} \times S_2(x_{EAN} = 1)$. This in turn allows determination of the effective solvation number

$$Z_{ib} = \frac{c_{AN} - c_{AN}^{app}}{c_{EAN}} \quad (6)$$

shown in Fig. 5b. At low IL content the obtained data exhibit a pronounced linear decrease from Z_{ib}^0 = 6.9 ± 0.2 at infinite dilution to ~2 at $x_{EAN} \approx 0.2$. Beyond this breakpoint Z_{ib} continues to decrease with significantly smaller slope. A similar behaviour was observed for the effective solvation numbers of 1-alkyl-3-methylimidazolium tetrafluoroborates in AN, which also drop from ~6–7 at $x_{IL} \to 0$ to ~2 at $x_{IL} \approx 0.2$.[13] For electrolyte solutions decreasing Z_{ib} with increasing salt concentration is common and explained in terms of solvation-shell overlap.[24,50] This certainly also applies to the dilute IL solutions. The breakpoint at $x_{EAN} \approx 0.2$ may be related to the pronounced formation of contact ion pairs (CIPs) for this system (see below) which should be associated with at least partial desolvation of the CIPs due to charge neutralization. This interpretation would explain, why the maximum of S_1 (ESI,† Table S2) and thus of the CIP concentration is at $x_{EAN} \approx 0.2$.

The infinite dilution value, Z_{ib}^0, is a measure of the strength of ion–solvent interactions and can be compared to coordination numbers from scattering experiments or computer simulations, as well as to other effective solvation numbers.[24] Apparently, no literature data for solvation numbers of EAN in AN are available but Perron *et al.*[15] concluded from the viscosity B parameter that ''electrostriction or coulombic solvation is the leading effect in AN'' (in contrast to the structure breaking effect claimed for aqueous solutions). Also, the present Z_{ib}^0 = 6.9 ± 0.2 is broadly compatible with values observed for alkaline ($Z_{ib}^0(LiClO_4^-)$ = 6.3; $Z_{ib}^0(NaClO_4^-)$ = 4.9) and alkaline earth perchlorates ($Z_{ib}^0(Mg(ClO_4)_2^-)$ = 9.9; $Z_{ib}^0(Ca(ClO_4)_2^-)$ = 6.9).[50] The latter data can be interpreted as cation solvation numbers as ClO_4^- was found to be unsolvated in AN.[51] No direct information on nitrate solvation is available but because of the small acceptor number of AN also only weak interactions with this anion are expected.[22,52] On the other hand, in addition to electrostatic ion–dipole interactions, also hydrogen bonding between $[EtNH_3]^+$ and the nitrile group of AN is possible, similar to what was observed for AN + water mixtures.[53,54] Thus, it appears reasonable to attribute also the present Z_{ib} values mainly to cation–solvent interactions.

From its definition Z_{ib} is the number of ''missing'' AN molecules per EAN ion pair, *i.e.* of solvent molecules that differ so much in their dynamics from ''free'' AN that they do not contribute to mode 2 anymore. The question then appears whether these solvent molecules interact so strongly with the ions that they are completely immobilized or just slowed down and therefore pop up as a new lower-frequency mode in the dielectric spectrum.[24] For the investigated AN + 1-alkyl-3-methylimidazolium tetrafluoroborate mixtures the latter was found, with the ''slow AN'' contribution accidentally overlapping with the IL mode.[13] However, for the present EAN + AN mixtures an analysis along the lines of ref. 13 yielded incompatible results. In particular, the derived ion-pair association constant was at variance with the literature (see below). Thus, we may conclude that $[EtNH_3]^+$–AN interactions are strong enough to immobilize the solvating molecules on the timescale probed by our dielectric spectra.

3.3 Lower frequency mode

3.3.1 Relaxation times. Although the $[EtNH_3]^+$ cation possesses a significant permanent dipole moment, its value of μ_+ = 3.9 D[55] is not sufficient to explain the pronounced maxima of ε_s (Fig. 3a) and S_1 (Fig. 7a). Therefore, similar to other IL + aprotic solvent mixtures,[11,13,42] the simultaneous presence of free cations and ion pairs can be reasonably assumed, although the individual contributions of both dipolar species to the dielectric spectra of the mixtures cannot be resolved. However, their existence is clearly manifested in the concentration dependence of relaxation time, τ_1 (Fig. 6a), and α_1 parameter (Fig. 3b) of mode 1. The initial increase of both quantities, with maxima at $x_{EAN} \approx 0.1$ and subsequent decrease indicates that the shape and the peak position of mode 1 are determined by the relative weights of the ion-pair and cation relaxations of (unknown) relaxation times τ_{IP} and τ_+ where $\tau_{IP} > \tau_1 > \tau_+$. The observed variation of τ_1 and α_1 can be rationalized as follows: As shown below ion pairs largely predominate at low x_{EAN}, thus a rather small α_1 with τ_1 dominated by the lower-frequency ion-pair relaxation. With increasing x_{EAN} the fraction of free cations increases, so that α_1 increases. As both relaxation times, τ_{IP} and τ_+, will increase with increasing viscosity τ_1 also increases despite growing cation contribution. At $x_{EAN} \approx 0.1$ ion-pair and cation contributions are comparable, thus maximum width of mode 1. For larger EAN mole fractions ion pairs re-dissociate and free cations become more and more important. Therefore, α_1 and τ_1 decrease again. This scenario of pronounced ion-pair

formation up to $x_{EAN} \approx 0.1$ followed by subsequent re-dissociation is supported by the initial strong decrease and subsequent plateau of the molar conductivity, Λ (for better comparison with corresponding relaxation times and viscosities normalized reciprocal molar conductivities, Λ_{EAN}/Λ, are shown in Fig. 6a). Note that the rather small relaxation times ($\tau_1 < 40$ ps, ESI,† Table S2) for $x_{EAN} \leq 0.4$, as well as the fact that ion-pair and cation modes could not be separated, indicate that the sizes of the cation and the formed ion pair are rather similar. This points to contact ion pairs (CIPs) as the dominating aggregate.

At $x_{EAN} \approx 0.5$ the strong increase of viscosity causes τ_1 to rise again and for $0.7 \leq x_{EAN} \leq 1$ the relaxation time is even proportional to viscosity (Fig. 6b). From the slope of τ_1 *vs.* η a friction coefficient of $C = 0.127$ can be calculated, which is close to that of neat EAN ($C = 0.091$), obtained from temperature-dependent measurements.[56] This implies that the dynamical properties of pure EAN are preserved down to a dilution of $x_{EAN} \approx 0.5$ (Fig. 6a) and suggests that AN acts as a "lubricant" accelerating the overall dynamics, similar to what was found for 1-alkyl-3-methylimidazolium IL + AN mixtures.[13] The similar friction coefficients also suggest that at least down to $x_{EAN} \approx 0.7$ the $[EtNH_3]^+$ cation relaxes *via* large-angle jumps as the pure IL.[26,38]

3.3.2 Amplitude. Using eqn (5) the conclusions made in Section 3.2.1 can be confirmed and extended quantitatively. Fig. 7a shows that, except for the most EAN-rich mixtures, cation relaxation alone cannot explain the amplitude of mode 1. With decreasing IL content the effective dipole moment, $\mu_{eff,EAN}$, calculated using eqn (5) from S_1 and the analytical EAN concentration, c_{EAN}, strongly increases from $\mu_{eff,EAN} = 4.8$ D, for pure EAN to 19.3 D at $x_{EAN} \rightarrow 0$ (Fig. 7b). This pronounced change of $\mu_{eff,EAN}$, together with the changes of τ_1 and α_1 at low x_{EAN} (Fig. 6), strongly hints at an equilibrium between free cations and EAN ion pairs.

Indeed, the $x_{EAN} = 1$ value (4.8 D) can be attributed to the effective dipole moment of the $[EtNH_3]^+$ cation,[26,38] $\mu_{eff,+}$, as it is in excellent agreement with semiempirical calculations[57] for this entity, yielding 4.9 D. Also, the infinite-dilution limit of $\mu_{eff,EAN}$ (19.3 D) is compatible with the dipole moment of a contact ion-pair (CIP) as semiempirical calculations[57] yielded 15.8 D and 18 D, depending on the relative orientations of NO_3^- and $[EtNH_3]^+$. For the solvent-shared ion pair (SIP) the considerably larger value of 40.1 D was obtained. The present $x_{EAN} \rightarrow 0$ limit of $\mu_{eff,EAN}$ also agrees well with the estimate of 16.3 D by Weingärtner *et al.*[58]

For mixtures of imidazolium ILs with AN $\mu_{eff,IL}$ values remained essentially equal to $\mu_{eff,+}$ down to $x_{IL} \approx 0.2$ before steeply increasing to $\mu_{eff,CIP}$ on further dilution. Together with other characteristic changes of the relaxation parameters this was attributed to a rather rapid transition of the dynamics from IL-like to electrolyte-solution-like behavior.[13] For EAN + AN the transition is much smoother. This observation, as well as the sharply increasing asymmetry of mode 1 (*i.e.* decreasing β_1, Fig. 3b) for $x_{EAN} \gtrsim 0.6$ may hint at microheterogeneities with AN-rich domains containing CIPs and EAN-rich domains showing the same dynamics as the pure IL. As strong hydrogen bonds between anions and cations are a dominant feature of pure EAN[5,38] such a hypothesis is supported by a comparison to mixtures of AN + water, where the formation of water clusters induced by hydrogen-bonding is well known.[53,59]

To account for the simultaneous contributions of CIPs and free dipolar cations to S_1 eqn (5) modifies to

$$S_1 = \frac{\varepsilon_s}{2\varepsilon_s + 1}\frac{N_A}{k_B T \varepsilon_0}\left[(c_{EAN} - c_{CIP})\mu_{eff,+}{}^2 + c_{CIP}\mu_{eff,CIP}{}^2\right] \quad (7)$$

where $c_{EAN} = c_+ + c_{CIP}$ is the total concentration of EAN, and c_+ and c_{CIP} are the concentrations of free cations and CIPs, respectively. Here it is assumed that dipole–dipole correlations between cations and ion pairs are negligible. At least for dilute solutions this should be reasonable so that the determined value of the standard-state association constant is not significantly affected.

Inserting the limiting values of $\mu_{eff,EAN}$, 4.8 D and 19.3 D, for $\mu_{eff,+}$ and $\mu_{eff,CIP}$ into eqn (7) then yields c_{CIP} and c_+, and thus the corresponding association constants

$$K_A = \frac{c_{CIP}}{(c_{EAN} - c_{CIP})^2} \quad (8)$$

shown in Fig. 8b. This, in turn, allows determination of the standard state association constant, K_A^0, by extrapolation with a Guggenheim-type equation[23]

$$\log K_A = \log K_A^0 - \frac{2A_{DH}\sqrt{I}}{1 + R_{ij}B_{DH}\sqrt{I}} + A_K I + B_K I^{3/2} \quad (9)$$

where $I(\equiv c_{EAN})$ is the stoichiometric (nominal) ionic strength. The required Debye–Hückel constants for the activity coefficients in AN, $A_{DH} = 1.643$ L$^{1/2}$ mol$^{-1/2}$ and $B_{DH} = 4.857 \times 10^9$ L$^{1/2}$ mol$^{1/2}$ m^{-1}, were calculated according to ref. 60. For the upper limit of ion association, $R_{ij} = 0.325$ nm, the MOPAC[57] value for the contact distance was used; A_K(= −2.149 L mol^{-1}) and B_K(= 0.5772 L$^{3/2}$ mol$^{-3/2}$) are empirical fit parameters.

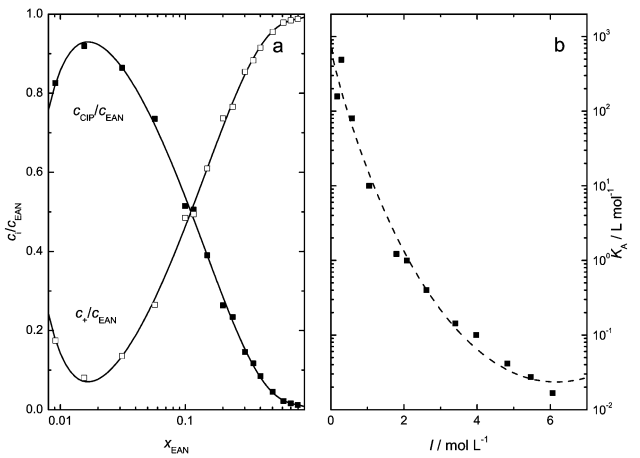

Fig. 8 (a) Relative concentrations of contact ion pairs, c_{CIP}/c_{EAN} (■) and $[EtNH_3]^+$, c_+/c_{EAN} (□). (b) Association constants, K_A (■) as a function of nominal ionic strength, I, at 25 °C. Solid lines (a) are visual guides; the dashed line (b) represents the fit with eqn (9).

Since dielectric spectra were only recorded for $c_{EAN} \geq 0.172$ mol L^{-1} the so extrapolated value of the standard-state equilibrium constant, $K_A^0 = (970 \pm 350)$ L mol^{-1}, is only an estimate. Nevertheless, it is in very good agreement with the value determined by Perron *et al.*[15] with dilute-solution conductivity measurements ($K_A^0 = 1094$ L mol^{-1}). Together with the inference from τ_1 (see above) this confirms CIPs as the predominating ion-pair species. The assumption of solvent-shared ion pairs would lead to unreasonably small K_A^0 but requires significantly larger τ_1. Unrealistic association constants were also obtained for the assumption that the bound solvent, corresponding to $Z_{ib} > 0$ derived from S_2, contributes to S_1.

Except may be for $[C_2mim][BF_4]$ ($K_A^0([C_2mim][BF_4]) = 245$ L mol^{-1}), which is probably an outlier when compared to the conductivity value,[13] the standard-state association constants found for 1-alkyl-3-methylimidazolium tetrafluoroborates in AN ($K_A^0([C_4mim][BF_4]) = 33.9$ L mol^{-1}; $K_A{}^0([C_6mim][BF_4]) = 9.77$ L mol^{-1}) are very similar to data for other 1 : 1 electrolytes in this solvent.[13] The large value of $K_A^0 = (970 \pm 350)$ L mol^{-1} for EAN, which even exceeds the association constants of 2 : 1 electrolytes by a factor of at least 2 ($K_A^0(Ca(ClO_4)_2) = 550$ L mol^{-1})[50] but generally 5,[50,61] is thus exceptional and indicates that Coulomb interactions are not the main driving force for EAN association in AN. This conclusion is supported by the prevalence of CIPs despite strong cation solvation. Keeping in mind the importance of hydrogen bonding for the properties of pure EAN[4,5,58] we may therefore safely conclude that strong hydrogen bonding between $[EtHN_3]^+$ and NO_3^- dominates ion–ion interactions in mixtures with AN and possibly also other dipolar aprotic solvents.

4 Concluding remarks

To some extent the dielectric relaxation behaviour of the present EAN + AN mixtures is reminiscent to that of AN + imidazolium tetrafluoroborate systems.[13] In particular, mixture dynamics has molten-salt character down to $x_{EAN} \approx 0.5$ with added AN acting as a ''lubricant'' for the collective translational and rotational motions. In this region only bound but no free AN molecules can be detected by DRS, in line with recent MD simulations and optical Kerr effect studies on $[C_5mim][NTf_2]$ + AN, showing AN dipoles oriented towards the imidazolium moiety of the cations.[62] With aprotic imidazolium ILs EAN also shares the smooth transition to electrolyte-solution behaviour at $x_{EAN} \approx 0.4$–0.5. What differs is the stronger cation–solvent interaction of $[EtNH_3]^+$, compared to imidazolium cations, as for the latter solvating AN molecules are only slowed down[13] but not frozen on the timescale of the present experiments. The major distinction between protic and aprotic ILs in mixtures with aprotic solvents (as far as the present results can be generalized) is the strong tendency of EAN to form CIPs, which seem to prevail to some extent even at $x_{EAN} > 0.5$ (Fig. 7).

It would be interesting to see how this combination of stronger cation solvation and H-bond driven CIP formation affects other mixture properties, in particular, solvation dynamics. In this area dielectric continuum models are known to work surprisingly well for polar liquids[63] and even for protic solvents like water.[64] Although the treatment of dc conductivity is still a matter of discussion, continuum models appear also to be suitable for aprotic ionic liquids.[28,65,66] For imidazolium ILs + water the situation is not so clear yet[67] as the experimental solvation response functions neither agree with a continuum treatment of the dielectric data nor with a more elaborate molecular model.[68]

From their structure acetonitrile, ethylammonium and nitrate are rather simple molecules/ions and thus within the reach of modern theoretical and simulation methods (although proper treatment of hydrogen bonding may be a problem). This makes EAN + AN a benchmark system for mixtures of protic ionic liquids with aprotic solvents. It is therefore hoped that the present dielectric relaxation study stimulates further experimental and theoretical research into the dynamics of such mixtures with potential practical interest.

Acknowledgements

The authors thank Prof. Dr W. Kunz for the provision of the laboratory facilities and the *Deutsche Forschungsgemeinschaft* for funding this work within the framework of Priority Program SPP 1191, ''Ionic Liquids''. V. N. acknowledges the *Deutscher Akademischer Austauschdienst (DAAD)* for financial support.

References

1 N. K. Plechkova and K. R. Seddon, *Chem. Soc. Rev.*, 2008, **37**, 123–150.
2 T. L. Greaves and C. J. Drummond, *Chem. Rev.*, 2008, **108**, 206–237.
3 J. Le Bideau, L. Viau and A. Vioux, *Chem. Soc. Rev.*, 2011, **40**, 907–925.
4 D. F. Evans and S.-H. Chen, *J. Am. Chem. Soc.*, 1981, **103**, 481–482.
5 K. Fumino, A. Wulf and R. Ludwig, *Angew. Chem., Int. Ed.*, 2009, **48**, 5184–5186.
6 D. F. Evans, *Langmuir*, 1988, **4**, 3–12.
7 T. L. Greaves, A. Weerawardena, I. Krodkiewska and C. J. Drummond, *J. Phys. Chem. B*, 2008, **112**, 896–905.
8 O. Zech, S. Thomaier, A. Kolodziejski, D. Touraud, I. Grillo and W. Kunz, *J. Colloid Interface Sci.*, 2010, **347**, 227–232.
9 H. Weingärtner, *Angew. Chem., Int. Ed.*, 2008, **47**, 654–670.
10 E. W. Castner and J. F. Wishart, *J. Chem. Phys.*, 2010, **132**, 120901.
11 J. Hunger, A. Stoppa, R. Buchner and G. Hefter, *J. Phys. Chem. B*, 2008, **112**, 12913–12919.
12 J. Hunger, A. Stoppa, S. Schrödle, G. Hefter and R. Buchner, *ChemPhysChem*, 2009, **10**, 723–733.
13 A. Stoppa, J. Hunger, G. Hefter and R. Buchner, *J. Phys. Chem. B*, 2012, **116**, 7509–7521.
14 M. Allen, F. Evans and R. Lumry, *J. Solution Chem.*, 1985, **14**, 549–560.
15 G. Perron, A. Hardy, J.-C. Justice and J. E. Desnoyers, *J. Solution Chem.*, 1993, **22**, 1159–1178.
16 A. J. Parker, *Pure Appl. Chem.*, 1981, **53**, 1437–1445.

17 A. Chu and P. Braatz, *J. Power Sources*, 2002, **112**, 236–246.
18 A. Stoppa, PhD thesis, Regensburg University, 2010.
19 T. Ohba and S. Ikawa, *Mol. Phys.*, 1991, **73**, 985–997.
20 J. Barthel and M. Kleebauer, *J. Solution Chem.*, 1991, **20**, 977–993.
21 P. Foggi, P. Bartolini, M. Bellini, M. G. Giorgini, A. Morresi, P. Sassi and R. S. Cataliotto, *Eur. Phys. J. D*, 2002, **21**, 143–151.
22 J. Barthel, M. Kleebauer and R. Buchner, *J. Solution Chem.*, 1995, **24**, 1–17.
23 R. Buchner, *Pure Appl. Chem.*, 2008, **80**, 1239–1252.
24 R. Buchner and G. Hefter, *Phys. Chem. Chem. Phys.*, 2009, **11**, 8984–8999.
25 D. A. Turton, J. Hunger, A. Stoppa, G. Hefter, A. Thoman, M. Walther, R. Buchner and K. Wynne, *J. Am. Chem. Soc.*, 2009, **131**, 11140–11146.
26 D. A. Turton, T. Sonnleitner, A. Ornter, M. Walther, G. Hefter, K. R. Seddon, S. Stana, N. Plechkova, R. Buchner and K. Wynne, *Faraday Discuss.*, 2012, **154**, 145–153.
27 F. O. Raineri and H. L. Friedman, *Adv. Chem. Phys.*, 1999, **107**, 81–189.
28 M. Maroncelli, X.-X. Zhang, M. Liang, D. Roy and N. P. Ernsting, *Faraday Discuss.*, 2012, **154**, 409–424.
29 A. Stoppa, O. Zech, W. Kunz and R. Buchner, *J. Chem. Eng. Data*, 2010, **55**, 1768–1773.
30 S. Shaukat and R. Buchner, *J. Chem. Eng. Data*, 2011, **56**, 4944–4949.
31 F. Kremer and A. Schönhals, *Broadband Dielectric Spectroscopy*, Springer, Berlin, 2003.
32 C. J. F. Böttcher and P. Bordewijk, *Theory of electric polarization*, Elsevier, Amsterdam, 1978, vol. 1 & 2.
33 J. Hunger, PhD thesis , Regensburg University, 2009.
34 T. Sonnleitner, D. Turton, S. Waselikowski, J. Hunger, A. Stoppa, M. Walther, K. Wynne and R. Buchner, *J. Mol. Liq.*, submitted.
35 S. Schrödle, G. Hefter, W. Kunz and R. Buchner, *Langmuir*, 2006, **22**, 924–932.
36 J. Barthel, K. Bachhuber, R. Buchner, H. Hetzenauer and M. Kleebauer, *Ber. Bunsen-Ges. Phys. Chem.*, 1991, **95**, 853–859.
37 D. Turton and K. Wynne, *J. Chem. Phys.*, 2008, **128**, 154516.
38 J. Hunger, T. Sonnleitner, L. Liu, R. Buchner, M. Bonn and H. J. Bakker, *J. Phys. Chem. Lett.*, 2012, **3**, 3034–3038.
39 C. Schröder, J. Hunger, A. Stoppa, R. Buchner and O. Steinhauser, *J. Chem. Phys.*, 2008, **129**, 184501.
40 C. Schröder and O. Steinhauser, in *Computational Spectroscopy: Methods, Experiments and Applications*, ed. J. Grünenberg, Wiley-VCH, Weinheim, Germany, 2010.
41 C. Schröder, T. Sonnleitner, R. Buchner and O. Steinhauser, *Phys. Chem. Chem. Phys.*, 2011, **13**, 12240–12248.
42 J. Hunger, A. Stoppa, R. Buchner and G. Hefter, *J. Phys. Chem. B*, 2009, **113**, 9527–9537.
43 S. H. Glarum, *J. Chem. Phys.*, 1960, **33**, 1371–1375.
44 B. Wurm, M. Münsterer, J. Richardi, R. Buchner and J. Barthel, *J. Mol. Liq.*, 2005, **119**, 97–106.
45 J. L. Dote and D. Kivelson, *J. Phys. Chem.*, 1983, **87**, 3889–3893.
46 R. Jellema, J. Bulthuis and G. van der Zwan, *J. Mol. Liq.*, 1997, **73**, 179–193.
47 J. Barthel, H.-J. Gores, G. Schmeer and R. Wachter, *Top. Curr. Chem.*, 1983, **111**, 33–144.
48 E. A. S. Cavell, P. C. Knight and M. A. Sheikh, *J. Chem. Soc., Faraday Trans.*, 1971, **67**, 2225–2233.
49 J. Barthel, H. Hetzenauer and R. Buchner, *Ber. Bunsen-Ges. Phys. Chem.*, 1992, **96**, 1424–1432.
50 P. N. Eberspächer, E. Wismeth, R. Buchner and J. Barthel, *J. Mol. Liq.*, 2006, **129**, 3–12.
51 J. Barthel and R. Deser, *J. Solution Chem.*, 1994, **23**, 1133–1146.
52 B. Clare, G. Hefter and P. Singh, *Aust. J. Chem.*, 1990, **43**, 257–261.
53 T. Takamuku, M. Tabata, A. Yamaguchi, J. Nishimoto, M. Kunamoto, H. Wakita and T. Yamaguchi, *J. Phys. Chem. B*, 1998, **102**, 8880–8888.
54 D. S. Venables and C. A. Schmuttenmaer, *J. Chem. Phys.*, 1998, **108**, 4935–4944.
55 E. I. Izgorodina, M. Forsyth and D. R. MacFarlane, *Phys. Chem. Chem. Phys.*, 2009, **11**, 2452–2458.
56 T. Sonnleitner, D. Turton, G. Hefter, A. Ortner, S. Waselikowski, M. Walther, K. Wynne and R. Buchner, in preparation.
57 J. J. P. M. Stewart, *Stewart Computational Chemistry*, Colorado Springs, CO, USA, 2009.
58 H. Weingärtner, A. Knocks, W. Schrader and U. Kaatze, *J. Phys. Chem. A*, 2001, **105**, 8646–8650.
59 E. M. Tee, A. Awichi and W. Zhao, *J. Phys. Chem. A*, 2002, **106**, 6714–6719.
60 J. O. Bockris and A. K. N. Reddy, *Modern Electrochemistry: Ionics*, Plenum Press, New York, 1998.
61 A. Apelblat, *J. Solution Chem.*, 2011, **40**, 1234–1257.
62 F. Bardak, D. Xiao, L. G. Hines, P. Son, R. A. Bartsch, E. L. Quitevis, P. Yang and G. A. Voth, *ChemPhysChem*, 2012, **13**, 1687–1700.
63 M. L. Horng, J. A. Gardecki, A. Papazyan and M. Maroncelli, *J. Phys. Chem.*, 1995, **99**, 17311–17337.
64 M. Sajadi, T. Obernhuber, S. A. Kovalenko, M. Mosquera, B. Dick and N. P. Ernsting, *J. Phys. Chem. A*, 2009, **113**, 44–55.
65 X.-X. Zhang, C. Schröder and N. P. Ernsting, *J. Chem. Phys.*, 2013, **138**, 111102.
66 X.-X. Zhang, M. Liang, N. P. Ernsting and M. Maroncelli, *J. Phys. Chem. Lett.*, 2013, **4**, 1205–1210.
67 X.-X. Zhang, M. Liang, J. Hunger, R. Buchner and M. Maroncelli, *J. Phys. Chem. B*, 2013, **117**, DOI: 10.1021/jp4043528.
68 S. Daschakraborty and R. Biswas, *J. Phys. Chem. B*, 2011, **115**, 4011–4024.

